ISSN 1063-7788, Physics of Atomic Nuclei, 2009, Vol. 72, No. 10, pp. 1629–1638. © Pleiades Publishing, Ltd., 2009.
Original Russian Text © O.V. Bespalova, I.N. Boboshin, V.V. Varlamov, T.A. Ermakova, B.S. Ishkhanov, E.A. Romanovsky, T.I. Spasskaya, T.P. Timokhina, 2009, published in Yadernaya Fizika, 2009, Vol. 72, No. 10, pp. 1686–1694.

NUCLEI
Experiment

# Investigation of the Shell Structure of $40 \leqslant A \leqslant 132$ Magic and Near-Magic Nuclei within the Mean-Field Model Involving a Dispersive Optical Potential

**O. V. Bespalova*, I. N. Boboshin, V. V. Varlamov, T. A. Ermakova, B. S. Ishkhanov, E. A. Romanovsky, T. I. Spasskaya, and T. P. Timokhina**

*Skobeltsyn Institute of Nuclear Physics, Moscow State University, Moscow, 119992 Russia*

Received December 25, 2008

**Abstract**—A method for determining parameters of a dispersive optical potential is presented. This method is aimed at calculating single-particle energies of neutron and proton states of magic and near-magic nuclei. It is based on the use of global parameters of the imaginary part of the traditional-optical-model potential and experimental data on single-particle energies in the vicinity of the Fermi surface that were determined by simultaneously evaluating data on nucleon-stripping and nucleon-pickup reactions on the same nucleus. The potential of the method for describing and predicting single-particle energies of $40 \leqslant A \leqslant 132$ magic and near-magic nuclei is demonstrated.

PACS numbers: 21.10.Pc
**DOI:** 10.1134/S1063778809100032

## 1. INTRODUCTION

The dispersive approach to determining the nucleon mean field unified for positive and negative energies [1] has been successfully used to analyze data on the scattering of nuclei and on their single-particle properties. This approach is based on a physically justified extrapolation of the parameters of the dispersive optical potential from the region $E > 0$ to the region $E < 0$. The real part of the dispersive optical potential consists of a component $V_{\rm HF}$ belonging to the Hartree–Fock type and depending smoothly on energy and a dispersive component $\Delta V$ depending sharply on energy in the vicinity of the Fermi energy $E_{\rm F}$. The dispersive component is calculated on the basis of data on the imaginary part of the potential; this imaginary part may be assumed to be symmetric with respect to $E_{\rm F}$ (see [1]) and must be known over a broad energy range. The parameters of the Hartree–Fock component are determined from a fit of the results of respective calculations to the empirical value of the energy $E_{\rm F}$ and (i) to the experimental cross sections for nucleon–nucleus scattering or (ii) to two radial moments of the real part of the phenomenological potential of the traditional (nondispersive) optical model (TOM). The first method is called the dispersive optical-model analysis (DOMA) (see [2]). The second is referred to as the variational moment approach (VMA) (see [1, 3]).

Both methods (VMA and DOMA) yield close results. In order to apply these methods, one needs experimental data on nucleon scattering over a broad energy range. It should be emphasized that the fact that the mean field for $E < 0$ is found on the basis data for $E > 0$, which are more extensive than data for $E < 0$, is one of the advantages of the dispersive approach. However, the range of nuclei for which experimental data on the scattering of nucleons on them are sufficient for implementing the DOMA and VMA methods is quite narrow. In particular, it obviously does not include unstable nuclei appearing as candidates for new magic nuclei, but investigations of such nuclei are very topical in contemporary nuclear physics. Moreover, it turns out that, upon an extrapolation of the component $V_{\rm HF}$ from the region $E > 0$ to the region $E < 0$, the error in the parameter characterizing the slope of the dependence $V_{\rm HF}(E)$ grows to such an extent that it begins to affect the calculation of single-particle energies $E_{nlj}$ of deeply lying states.

In order to address the problem of studying single-particle properties for a wide range of nuclei, including unstable neutron-rich and neutron-deficient nuclei, one needs a method that would make it possible to construct a dispersive optical potential, but which would not require the presence of experimental data on nucleon scattering over a broad interval of energies and within which one could determine the parameters

*E-mail: besp@hep.sinp.msu.ru

of the component $V_{\rm HF}$ on the basis of data on single-particle properties of nuclei.

Until recently, the errors in the values of $E_{nlj}$ in the vicinity of $E_{\rm F}$ that were determined from data on nucleon-stripping or nucleon-pickup reactions were 20 to 30%. At such errors, it was meaningless to aim at developing a method for constructing a dispersive optical potential intended for calculating single-particle properties of nuclei. The method developed in [4] for matching data on nucleon-stripping and nucleon-pickup reactions on the same nucleus (for the sake of brevity, we will refer to it in the following as the matching method)—a similar method was independently proposed later in [5]—made it possible to reduce the errors in $E_{nlj}$ near $E_{\rm F}$ to 10%, thereby opening new possibilities for developing the dispersive approach to determining nuclear mean fields.

In this study, we present a method intended for constructing a dispersive optical potential and aimed at calculating single-particle properties of nuclei, including unstable neutron-rich and neutron-deficient nuclei. With the aid of this method, we calculate the single-particle energies $E_{nlj}$ of $40 \leqslant A \leqslant 132$ magic and near-magic nuclei. In this way, experimental data obtained by the matching method were well described within their errors.

## 2. METHOD FOR CONSTRUCTING DISPERSIVE OPTICAL POTENTIALS

Since the dispersion component of the real part of the dispersive optical potential is calculated on the basis of data on its imaginary part, a determination of this imaginary part is the first step in constructing the dispersive optical potential. The fact that the imaginary part of the dispersive optical potential is symmetric with respect to the Fermi energy $E_{\rm F}$ is its important property justified empirically. Since the dispersive optical potential describes states of the $A+1$ (particle states) and $A-1$ (hole states) systems, the energy $E_{\rm F}$ of the $n, p+A$ system can be represented as the half-sum

$$E_{\rm F} = (E_+ + E_-)/2, \qquad (1)$$

where $E_+$ is the energy of the first particle state (the most strongly bound and predominantly unfilled orbit) and $E_-$ is the energy of the last hole state (the most loosely bound and predominantly filled orbit). For the energies $E_+$ and $E_-$, we take here the experimental values of $E_{nlj}$ that were obtained by the matching method for the corresponding states. In case where it is difficult to single out states that can be treated as the first particle state and the last hole state according to the terminology adopted above, one can employ the respective formula of Bardeen–Cooper–Schrieffer (BCS) theory in determining the Fermi energy $E_{\rm F}$. This formula makes it possible to describe the shape of the Fermi surface and has the form

$$N_{nlj} = \frac{1}{2}\left(1 - \frac{(E_{nlj} - E_{\rm F})}{\sqrt{(E_{nlj} - E_{\rm F})^2 + \Delta^2_{\rm BCS}}}\right), \qquad (2)$$

where $\Delta_{\rm BCS}$ is the gap parameter. For this, we take here data obtained by the matching method for $N^{\rm expt}_{nlj}$ and $E^{\rm expt}_{nlj}$.

The method used here to construct the dispersive optical potential is based on the possibility of fixing a number of parameters of the potential (first of all, its imaginary part) in accordance with the predictions of systematics of global parameters of the traditional optical model. At the present time, the systematics proposed by Koning and Delaroche in [6] (in the following, the KD systematics) is thought to be the most reliable systematics of global parameters of the traditional optical model. This systematics was determined in analyzing a vast experimental database of cross sections for the elastic scattering and polarization of protons and neutrons, as well as total neutron-interaction cross sections. It is applicable to evaluating data on the scattering of 1-keV to 200-MeV nucleons by spherical nuclei of mass number $A$ between 24 and 209 and nuclei close to them. The strength parameters of the potential components depend smoothly on the energy, mass number, and relative neutron excess. The imaginary part of the potential depends on energy in the form that assumes that it is symmetric with respect to the Fermi energy. This makes it possible to use this imaginary part directly in analytic calculations of dispersive components.

The use of a more extensive experimental database—first of all, data on total neutron-interaction cross sections—distinguishes the KD systematics from the CH89 systematics proposed in [7] and employed earlier. In contrast to the KD systematics, the CH89 systematics requires changing the diffuseness parameter of the imaginary part of the potential, $a_s = a_d$, in order to match the results of the calculations with precision data obtained later for total proton reaction cross sections $\sigma_r$ [8]. In [9], it was shown that agreement between the calculated and measured values of $\sigma_r$ is attained upon reducing the value of $a_s^{\rm CH89} = a_d^{\rm CH89} = 0.69$ fm to the value of $a_s^{\rm CH89^*} = a_d^{\rm CH89^*} = 0.63$ fm, these values being averaged over the nuclei under study. For a large number of nuclei, local (individual for a specific $p+A$ system) values of $a_s^{\rm CH89^*} = a_d^{\rm CH89^*}$, which correlated with special features of the shell structure of nuclei (the values of $a_s^{\rm CH89^*} = a_d^{\rm CH89^*}$ were smaller for magic

than for nonmagic nuclei), were also found in that study. In addition, the statement that it is legitimate to equate the diffuseness parameter of the imaginary part of the neutron potential to the $a_s^{\mathrm{CH89}^*} = a_d^{\mathrm{CH89}^*}$ values found for protons was proven there.

The strength parameters of the volume ($W_s$) and surface ($W_d$) components of the imaginary part of the potential in the KD systematics depend on energy, the exponent in this dependence being $n = 2$:

$$W_s(E) = w_1 \frac{(E - E_\mathrm{F})^2}{(E - E_\mathrm{F})^2 + w_2^2}, \qquad (3)$$
$$W_d(E) = d_1 \frac{(E - E_\mathrm{F})^2 \exp[-d_2(E - E_\mathrm{F})]}{(E - E_\mathrm{F})^2 + (d_3)^2}.$$

We recall that the theory of infinite Fermi systems predicts a quadratic dependence of the imaginary part of the nuclear potential on energy. As was indicated above, the imaginary part from the KD systematics may directly be used to calculate the dispersion components of the dispersive optical potential. In the present study, we nevertheless employ the dependence (see [1])

$$J_{I,s}(E) = \alpha \frac{(E - E_0)^n}{(E - E_0)^n + \beta_{Is}^n}, \qquad (4)$$
$$J_d(E) = J_I(E) - J_s(E),$$

where $n = 4$ and $J_{I,s,d}$ are the volume integrals of ($I$) the total imaginary part of the dispersive optical potential and of its ($s$) volume and ($d$) surface components. The energy $E_0$ determines the interval between $2E_F - E_0$ and $E_0$ within which it would be reasonable to equate the imaginary part to zero. Frequently, the value of $E_0$ is equated to the Fermi energy $E_\mathrm{F}$. In a number of cases, agreement between $E_{nlj}^{\mathrm{DOP}}$ and $E_{nlj}^{\mathrm{expt}}$ is improved in the case of $E_0 \neq E_\mathrm{F}$ owing to more precisely specifying the dependence $J_I(E)$. Our experience shows that, in order to describe single-particle energies, the value of $n = 4$ is preferable in many cases to the value of $n = 2$. The most probable reason for this is that, in the vicinity of $E_\mathrm{F}$, the dependence in (4) at $n = 4$ leads to smaller values of the imaginary part than the respective dependence at $n = 2$. This complies to a greater extent with the idea that the imaginary part for states in the vicinity of $E_\mathrm{F}$ is close to zero.

Thus, a determination of the imaginary part of the dispersive optical potential reduces to finding the parameters $\alpha$ and $\beta_{I,s}$, as well as the radius and diffuseness parameters of the Woods–Saxon form of its volume ($r_s$ and $a_s$) and surface ($r_d$ and $a_d$) components.

In the present study, the parameter $\alpha$ in the dependence specified by Eq. (4) is determined with the aid of the KD systematics, namely,

$$\alpha = \left\langle J_I^{\mathrm{KD}} \right\rangle_{40-60\ \mathrm{MeV}}, \qquad (5)$$

where $\left\langle J_I^{\mathrm{KD}} \right\rangle_{40-60\ \mathrm{MeV}}$ is the value obtained by averaging, over the energy range between 40 and 60 MeV, the volume integral of the total imaginary part of the KD potential.

The parameter $\beta_s$ is determined from the condition requiring that $J_s(E_k)$ in (4) be equal to $J_s^{\mathrm{KD}}(E_k)$ at an energy $E_k$ such that $J_s^{\mathrm{KD}}(E_k) = \alpha/2$ [that is, when $J_s^{\mathrm{KD}}$ reaches approximately half the height of $J_I^{\mathrm{KD}}(\mathrm{E})$]:

$$\alpha \left[ 1 + \left( \frac{\beta_s}{(E_k - E_\mathrm{F})} \right)^4 \right]^{-1} = \frac{\alpha}{2}. \qquad (6)$$

From here, we obtain

$$\beta_s = E_k - E_\mathrm{F}. \qquad (7)$$

The parameter $\beta_I$ can be estimated by using the empirical values of $J_I(E_k)$ in the range $E_k < 20$ MeV or (in the case where such values are not available) the values of $J_I^{\mathrm{KD}}(E)$ in the range $E < 20$ MeV. Within the method developed in the present study and intended for calculating single-particle properties of nuclei, the parameter $\beta_I$ is free. Its optimum value is determined as that which minimizes the functional

$$\chi^2 = \frac{1}{N} \sum \frac{(E_{nlj}^{\mathrm{DOP}} - E_{nlj}^{\mathrm{expt(ev)}})^2}{\Delta^2}, \qquad (8)$$

where $E_{nlj}^{\mathrm{DOP}}$ are calculated single-particle energies, $E_{nlj}^{\mathrm{expt(ev)}}$ are their experimental or evaluated (in the absence of experimental data) counterparts, $N$ is the number of values of $E_{nlj}^{\mathrm{expt(ev)}}$, and $\Delta$ is the error in $E_{nlj}^{\mathrm{expt(ev)}}$. The optimum value of $\beta_I$ is found by the mesh-search method.

Within the method used here, the parameters $r_s$, $a_s$, $r_d$, and $a_d$ are borrowed from systematics of global parameters of the traditional-optical-model potential—namely, the KD systematics. Thus, the parameter $\beta_I$ is the only free parameter of the imaginary part of the dispersive optical potential. The strength parameter of the Hartree–Fock component of the dispersive optical potential is assumed to be smoothly dependent on energy. Its energy dependence can be represented in the form of an exponential function,

$$V_{\mathrm{HF}}(E) = V_{\mathrm{HF}}(E_\mathrm{F}) \exp\left( \frac{-\gamma(E - E_\mathrm{F})}{V_{\mathrm{HF}}(E_\mathrm{F})} \right), \qquad (9)$$

or in the form of a superposition of a linear and an exponential function,

$$V_{\rm HF}(E) = V_{\rm HF}(E_{\rm F}) - \lambda(E - E_{\rm F}), \quad E \leqslant E_{\rm F}; \qquad (10)$$

$$V_{\rm HF}(E) = V^1_{\rm HF}(E_{\rm F}) + V^2_{\rm HF}(E_{\rm F}) \exp\left[\frac{-\lambda(E - E_{\rm F})}{V^2_{\rm HF}(E_{\rm F})}\right], \quad E \geqslant E_{\rm F};$$

$$V_{\rm HF}(E_{\rm F}) = V^1_{\rm HF}(E_{\rm F}) + V^2_{\rm HF}(E_{\rm F}).$$

Thus, the Hartree–Fock component of the dispersive optical potential is determined by the parameters $V_{\rm HF}(E_{\rm F})$ [$V^1_{\rm HF}(E_{\rm F})$ and $V^2_{\rm HF}(E_{\rm F})$] and $\gamma(\lambda)$ for the dependence in (9) [or in (10)], the radius $r_{\rm HF}$, and the diffuseness parameter $a_{\rm HF}$.

The calculations show that the energy $E^{\rm DOP}_{1s_{1/2}}$ is highly sensitive to the choice of values for the parameter $\gamma(\lambda)$, which characterizes the slope of the dependence $V_{\rm HF}(E)$ in (9) [or in (10)]. If we determined this parameter on the basis of data on nucleon scattering for $E > 0$ and data on $E^{\rm expt(ev)}_{nlj}$ in the vicinity of $E_{\rm F}$, the error in it would lead to a sizable deviation of $E^{\rm DOP}_{1s_{1/2}}$ from the respective experimental values. This is the reason why, within the method developed here in order to construct the dispersive optical potential, the parameters $\gamma$ and $\lambda$ are found on the basis of data on $E^{\rm expt,ev}_{1s_{1/2}}$:

$$\gamma = \frac{V_{\rm HF}(E_{\rm F})}{E_{\rm F} - E_{1s_{1/2}}} \ln\left[\frac{V_{\rm HF}(E_{1s_{1/2}})}{V_{\rm HF}(E_{\rm F})}\right], \qquad (11)$$

$$\lambda = \frac{V_{\rm HF}(E_{1s_{1/2}}) - V_{\rm HF}(E_{\rm F})}{E_{\rm F} - E_{1s_{1/2}}}. \qquad (12)$$

For $E^{\rm expt}_{1s_{1/2}}$, we use here experimental data obtained in [10, 11] for relevant $(p, pn)$ and $(p, 2p)$ reactions. High-precision experimental information about the energies and widths of deep-lying neutron and proton states is presented in those articles for a large number of nuclei, including $^{40}$Ca, $^{90}$Zr, and $^{208}$Pb. In constructing the dispersive optical potential of nuclei for which there are no data on $E^{\rm expt}_{1s_{1/2}}$, use is made of the evaluated energy of the $1s_{1/2}$ state. Frequently, this evaluation is performed by the extrapolation method, in which case the regularities of the mass dependence of $E_{1s_{1/2}}$ that are predicted by the calculations in [12] on the basis of the relativistic mean-field model are taken into account.

The parameter $V_{\rm HF}(E_{\rm F})$ is found from a fit to $E_{\rm F}$; it can be represented in the form of the half-sum

$$V_{\rm HF}(E_{\rm F}) = \frac{V(E_+) + V(E_-)}{2}, \qquad (13)$$

where $V(E_+)$ and $V(E_-)$ are the strength parameters of the real potential, which describe the experimental values of the energies $E_+$ and $E_-$.

In the dispersive approach, the entire energy dependence of the potential components is concentrated in their strength parameters, the geometric parameters being energy-independent. This simplifies the calculation of the dispersive components and complies with the modern ideas of the dependence of the optical-potential parameters on the energy, mass number, and relative neutron excess (see, for example, the KD systematics). Therefore, averaged values are used for the parameters $r_{\rm HF}$ and $a_{\rm HF}$ within the DOMA and VMA methods and within the method proposed in the present study, since data on nucleon–nucleus scattering, empirical data on the volume integrals of the optical potential, and data on single-particle energies are described most precisely with them.

The spin–orbit potential is the most uncertain part of the optical potential. Calculations revealed that, without a significant loss of accuracy in $E^{\rm DOP}_{nlj}$, we can take, for the average parameters $r_{\rm so}$ and $a_{\rm so}$, the corresponding average parameters from the KD or the CH89 systematics and treat the parameter $V_{\rm so}$ as an adjustable one. The range parameter of the Coulomb potential in the form of that for a uniformly charged sphere can also be borrowed from the aforementioned systematics.

In practice, the procedure used here to construct the dispersive optical potential reduces to the following steps:

(i) On the basis of available experimental data, one determines the Fermi energy $E_{\rm F}$.

(ii) With the aid of the KD (or CH89*) systematics, one determines the parameters $\alpha$, $\beta_s$, $r_s$, $a_s$, $r_d$, $a_d$, $r_{\rm so}$, $a_{\rm so}$, and $r_{\rm C}$ and fixes them as average ones.

(iii) With some chosen trial values of the parameters $\beta_I$ and $V_{\rm so}$ and the input values of the parameters $r_{\rm HF}$ and $a_{\rm HF}$ for the states of energy $E_+$, $E_-$, and $E^{\rm expt,ev}_{1s_{1/2}}$, one solves the Schrödinger equation with the potential

$$-V(r, E_{nlj}) = V_{\rm HF}(r, E_{nlj}) + \Delta V_s(r, E_{nlj}) + \Delta V_d(r, E_{nlj}) + V_{\rm so}(r, E_{nlj}) - V_{\rm C}(r). \qquad (14)$$

From the conditions $E_{nlj} = {\rm E}_+, E_-$, and $E^{\rm expt,ev}_{1s_{1/2}}$, one finds the values of $V_{\rm HF}(E_{\rm F})$ (12) and $V_{\rm HF}(E_{1s_{1/2}})$ and then determines the parameter $\gamma(\lambda)$.

(iv) With the values found for the parameters $V_{\rm HF}(E_{\rm F})$ and $\gamma(\lambda)$, one again solves the Schrödinger equation for states for which there are experimental

data on $E_{nlj}^{\mathrm{expt}}$. For the energy-dependent real part of the dispersive optical potential, one selects a value of $E$ such that the absolute value $|E_{nlj}(E) - E|$, where $E_{nlj}(E)$ is a solution to the respective eigenvalue problem, does not exceed 10 keV. After that, one calculates the value of $\chi^2$ in (8) with values found for the energies $E_{nlj}^{\mathrm{DOP}} = E_{nlj}(E)$.

(v) Following the procedure of the mesh-search method, one then chooses different values of the parameters $r_{\mathrm{HF}}$ and $a_{\mathrm{HF}}$ and repeats the calculations outlined in items (iii) and (iv). The analogous procedure [items (iii) and (iv)] is also repeated at different values of $\beta_I$ and $V_{\mathrm{so}}$. As a result, one arrives at optimum values of the parameters $\beta_I$, $V_{\mathrm{HF}}(E_{\mathrm{F}})$, $\gamma(\lambda)$, $r_{\mathrm{HF}}$, $a_{\mathrm{HF}}$, and $V_{\mathrm{so}}$, those that minimize the functional $\chi^2$ in (8).

In relation to the DOMA and VMA approaches, the method proposed here for determining the parameters of the dispersive optical potential is aimed to a greater extent at describing single-particle energies, since some of its parameters are determined by minimizing the functional $\chi^2$ in (8) with respect to them.

In single-particle spectra, the particle–hole energy gap $\Delta$ between the first particle state and the last hole state is wider in traditional magic nuclei than in their neighbors. A large gap $\Delta$ is also expected for new magic nuclei. The method developed for constructing the dispersive optical potential is used here to analyze the dynamics of single-particle spectra in the $n + {}^{40,42,44,46,48,50,52,54,56}\mathrm{Ca}$, ${}^{46,48,50}\mathrm{Ti}$, ${}^{50,52,54}\mathrm{Cr}$, ${}^{54,56,58}\mathrm{Fe}$, ${}^{56}\mathrm{Ni}$, ${}^{84,86,88}\mathrm{Sr}$, ${}^{90,92,94,96}\mathrm{Zr}$, and ${}^{100,112,116,118,120,124,132}\mathrm{Sn}$ and $p + {}^{50,52}\mathrm{Cr}$, ${}^{54,56}\mathrm{Fe}$, and ${}^{90,92,94,96}\mathrm{Zr}$ systems in response to changes in $N$ and $Z$. Below, we present results obtained by means of the method proposed for determining the parameters of the dispersive optical potential.

## 3. RESULTS

### $n + {}^{40,42,46,48,50,52,54,56}$*Ca Systems*

The doubly magic nucleus ${}^{40}\mathrm{Ca}$ is one of the nuclei used as a testing ground for developing various procedures for constructing the dispersive optical potential via analyzing data on scattering and single-particle properties (see [13]). The addition of eight neutrons to ${}^{40}\mathrm{Ca}$ leads to the formation of another traditional doubly magic isotope, ${}^{48}\mathrm{Ca}$. For this calcium isotope, which is the last stable one, the excitation energy of the $2_1^+$ state—one of the magicity signatures—is 3.832 MeV. After decreasing to 1.026 MeV for ${}^{50}\mathrm{Ca}$, the energy $E_{2_1^+}$, begins to grow again, reaching 2.563 MeV for ${}^{52}\mathrm{Ca}$. Within the multiparticle shell model (MSM) [14], it is predicted that, in the isotope ${}^{54}\mathrm{Ca}$, the energy $E_{2_1^+}$ reaches a maximum value (approximately equal to that in ${}^{48}\mathrm{Ca}$). In that nucleus, the $2p_{3/2}$ and $2p_{1/2}$ neutron states are filled; also, a rather wide gap $\Delta$ between the $2p_{1/2}$ and $1f_{5/2}$ levels is formed. These properties of ${}^{54}\mathrm{Ca}$ give sufficient grounds to believe that this nucleus is a candidate for a doubly magic nucleus.

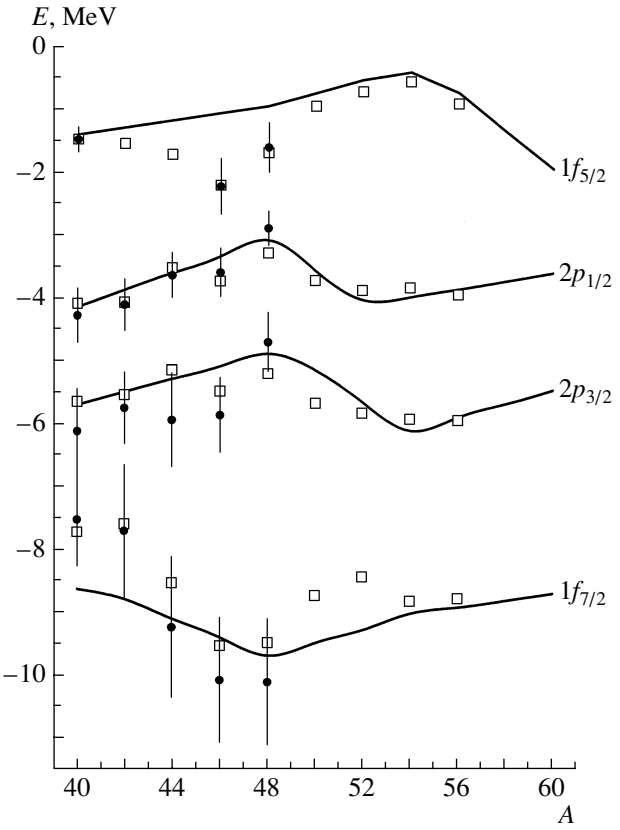


**Fig. 1.** Single-particle energies of neutron states in ${}^{40,42,44,46,48,50,52,54,56}\mathrm{Ca}$ nuclei: (solid curve) $E_{nlj}^{\mathrm{MSM}}$, (closed circles) $E_{nlj}^{\mathrm{expt}}$, and (open boxes) $E_{nlj}^{\mathrm{DOP}}$.

In order to construct the neutron dispersive optical potential for nuclei of the isotopic chain ${}^{40,42,46,48,50,52,54,56}\mathrm{Ca}$, we used data obtained by the matching method for $E_{nlj}^{\mathrm{expt}}$ in the vicinity of the Fermi energy $E_{\mathrm{F}}$ for neutron states of the stable isotopes ${}^{40,42,44,46,48}\mathrm{Ca}$ [15] and the values of $E_{1s_{1/2}}^{\mathrm{expt}}$ [10] for ${}^{40}\mathrm{Ca}$. For all isotopes under study, the energy of the $1s_{1/2}$ state was evaluated as $E_{1s_{1/2}}^{\mathrm{expt}}$ for ${}^{40}\mathrm{Ca}$; that is, $E_{1s_{1/2}}^{\mathrm{ev}} = -61.5$ MeV. The values calculated for the energy of this state within the relativistic mean-field model [12], which change insignificantly in response to a change in the mass number $A$ of the isotopes under study, furnished a sufficient motivation for this.

The calculations revealed that an increase in the gap $\Delta$ between the $2p_{1/2}$ and $1f_{5/2}$ neutron subshells of $^{54}$Ca in agreement with the predictions of the multiparticle shell model can be obtained via an increase of about 10% in the parameters $a_{\mathrm{HF}}$ and $V_{\mathrm{so}}$ in relation to the neighboring isotopes. Figure 1 shows the mass dependences of the energies $E_{nlj}^{\mathrm{expt}}$, $E_{nlj}^{\mathrm{MSM}}$, and $E_{nlj}^{\mathrm{DOP}}$ in the vicinity of $E_{\mathrm{F}}$ for the $1f_{7/2,5/2}$ and $2p_{3/2,1/2}$ neutron states of the $^{40,42,46,48,50,52,54,56}$Ca nuclei. From this figure, one can see that the values of $E_{nlj}^{\mathrm{DOP}}$ agree with $E_{nlj}^{\mathrm{expt}}$ within the errors in them for stable isotopes, as well as with the predictions $E_{nlj}^{\mathrm{MSM}}$ for unstable isotopes. This figure shows clearly the formation of the maximum gaps $\Delta$ between the $1f_{7/2}$ and $2p_{3/2}$ states in the doubly magic nucleus $^{48}$Ca and between the $1f_{5/2}$ and $2p_{1/2}$ states in the $^{54}$Ca nucleus, which is a candidate for a doubly magic nucleus.

Below, we illustrate the potential of the proposed method for determining the parameters of the dispersive optical potential in describing the dynamics of the formation of single-particle spectra of $20 \leqslant Z \leqslant 28$ nuclei in response to the change in the number of neutrons around the magic number of $N = 28$ ($1f$- to $2p$-shell nuclei).

### $20 \leqslant Z \leqslant 28$ *Nuclei in Which N Is Close to 28*

A systematic investigation of isotopic and isotonic dependences of the experimental values $E_{nlj}^{\mathrm{expt}}$ obtained by the matching method for neutron and proton states of $^{48}$Ca, $^{46,48,50}$Ti, $^{50,52,54}$Cr, and $^{54,56,58}$Fe was performed in [16]. A similar investigation was performed there for such states in the $^{56}$Ni nucleus that were determined from the scheme of decay of neighboring nuclei [17]. In particular, it was found that the isotonic dependences for the $1f_{7/2}$, $2p_{3/2}$, $2p_{1/2}$, and $1f_{5/2}$ states in the nuclei subjected to study and characterized by $N = 26$ and $N = 28$ can be described by a linear function featuring a coefficient that depends on a specific state, but which does not depend on $N$. For the nuclei being studied, single-particle energies of a number of states for which these energies could not be determined by the matching method because of the shortage of data on nucleon-stripping and nucleon-pickup reactions were evaluated with the aid of the aforementioned dependences. The energies evaluated in this way and used as a supplement to the experimental energy values made it possible to trace the pattern of changes in the single-particle spectra in response to changes in $N$ and $Z$—in particular, the formation of maximum gaps $\Delta$ as the numbers $N$ and $Z$ reach their magic value of 28.

Data on $E_{nlj}^{\mathrm{expt,ev}}$ were analyzed on the basis of the mean-field model featuring the dispersive optical potential by using the method for determining its parameters that was proposed in the present study. The evaluated energy of $E_{1s_{1/2}}^{\mathrm{ev}} = -62$ MeV for neutron states and the evaluated energy of $E_{1s_{1/2}}^{\mathrm{ev}} = -54$ MeV for proton states in $20 \leqslant Z \leqslant 28$ nuclei in which $N$ is close to 28 were obtained by using experimental data from [10] and results based on the relativistic mean-field model [12]. The energies $E_{nlj}^{\mathrm{DOP}}$ calculated with the values found for the parameters of the dispersive optical potential could be matched with $E_{nlj}^{\mathrm{expt,ev}}$ within the errors in the latter. The energies $E_{nlj}^{\mathrm{DOP}}$ for neutron and proton states of nuclei from the region $20 \leqslant Z \leqslant 28$ at $N$ in the vicinity of 28 are given in, respectively, Tables 5 and 6 from [16] along with $E_{nlj}^{\mathrm{expt,ev}}$.

### $n + ^{84,86,88}$*Sr and* $n, p + ^{90,92,94,96}$*Zr Systems*

In the isotopic chains $^{84,86,88}$Sr and $^{90,92,94,96}$Zr, the $^{88}$Sr and $^{90}$Zr nuclei are traditional nuclei that are magic in the number of neutrons and in which $N = 50$. Investigation of single-particle spectra for the isotopic chains of strontium and zirconium makes it possible to trace the dynamics of the formation of the energy gap $\Delta$ for $N = 50$ nuclei. Data obtained for $E_{nlj}^{\mathrm{expt}}$ and $N_{nlj}^{\mathrm{expt}}$ in [18, 19] by the matching method for the $n + ^{84,86,88}$Sr and $n, p + ^{90,92,94,96}$Zr systems demonstrated this dynamics and made it possible to discover magic properties of the $^{96}$Zr nucleus, consolidating the status of this nucleus as a candidate for new nuclei that are magic in the number of neutrons. Data on $E_{nlj}^{\mathrm{expt}}$ for neutron states in the $^{84,86,88}$Sr isotopic chain are indicative of an increase in the energy gap $\Delta$ between the $1g_{9/2}$ state, which is the last hole neutron state, and the $2d_{5/2}$ state, which is the first particle neutron state, as one approaches the magic nucleus $^{88}_{38}\mathrm{Sr}_{50}$. According to the results obtained by the matching method, the occupation probabilities for the $1g_{9/2}$ and $2d_{5/2}$ states are 0.97(3) and 0.04(2), respectively. Thus, the $1g_{9/2}$ state is almost filled, while the $2d_{5/2}$ state is nearly free. In the isotopes $^{84}$Sr and $^{86}$Sr, the $1g_{9/2}$ state is filled incompletely, its occupation probabilities being $N_{1g_{9/2}}^{\mathrm{expt}} = 0.58(6)$ and 0.78(8), respectively. In determining the Fermi energy $E_{\mathrm{F}}$ for these nuclei, we therefore used formula (2) of Bardeen–Cooper–Schrieffer theory. Agreement between the energies $E_{nlj}^{\mathrm{DOP}}$ calculated with the values found for the parameters of the dispersive optical potential and respective experimental data within the

errors in them was attained in [18] for the $^{84,86,88}$Sr nuclei.

In just the same way as $^{40}$Ca, the $^{90}_{40}Zr_{50}$ nucleus, which is a traditional magic nucleus in the number of neutrons, was also used as a testing ground for demonstrating the potential of the dispersive approach in determining the mean field (see, for example, [20]). Experimental data obtained in [19] by the matching method demonstrate how the filling of the $2d_{5/2}$ neutron subshell occurs as the number of neutrons increases in the $^{90,92,94,96}$Zr isotopic chain. In accord with the predictions of the single-particle shell model, this subshell proves to be completely filled in the $^{96}$Zr nucleus. Concurrently, the $2d_{5/2}$ subshell goes down, and this leads to an increase in the energy gap $\Delta$ between it and the free subshell $3s_{1/2}$. As a result, the structure of an individual shell, $2d_{5/2}$, is formed. This fact can be considered as a signature of the magicity of the $^{96}$Zr nucleus (so-called magic pair of numbers $N = 56$ and $Z = 40$). It is noteworthy that the process of separation of the $2d_{5/2}$ subshell in the $^{96}$Zr nucleus is similar to the process involving the separation of the $1f_{7/2}$ subshell in calcium isotopes and leading to the emergence of the traditional magic number $N = 28$.

The filling of the $2d_{5/2}$ neutron subshell in the $^{96}$Zr nucleus is accompanied by the rearrangement of the proton structure of the nucleus. As a result, the occupation probability $N_{nlj}$ for the $2p_{1/2}$ state, which is the last hole state, increases to 0.81(5) in $^{96}$Zr, while the occupation probability for the $1g_{9/2}$ state, which is the first particle state, decreases to 0.1 in $^{90,92,94}$Zr and to zero in $^{96}$Zr. This is how the change in the neutron structure of zirconium isotopes in response to an increase in $N$ affects their proton structure.

In constructing the neutron and proton dispersive optical potential for the isotopes $^{90,92,94,96}$Zr in order to determine the parameters $\gamma$ and $\lambda$ for the $n$, $p+$ $^{92,94,96}$Zr systems, we took here the values $E^{\rm expt}_{1s_{1/2}}$ from [11] for $^{90}$Zr, since the calculations of single-particle energies of nucleon states in $Z \approx 50$ nuclei on the basis of the relativistic mean-field model [12] showed that, in response to the change of six in the number of neutrons in a fixed-$Z$ nucleus, the energy $E_{1s_{1/2}}$ changes within 1 MeV. This value of $E^{\rm expt}_{1s_{1/2}}$ is within the experimental errors for $^{90}$Zr [11]. Agreement between the energies $E^{\rm DOP}_{nlj}$ calculated for neutron and proton states in $^{90,92,94,96}$Zr with the values found for the parameters of the dispersive optical potential and relevant experimental data within the errors in these data was attained in [19]. By way of illustration, the $E^{\rm DOP}_{nlj}$ values are contrasted in Fig. 2 against $E^{\rm expt}_{nlj}$ in the vicinity of $E_{\rm F}$ for neutron states of $^{90,92,94,96}$Zr.

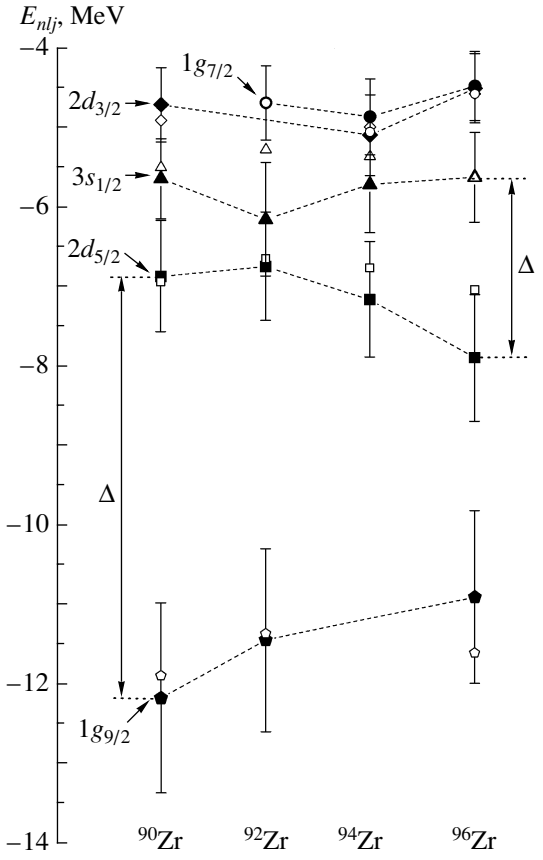


**Fig. 2.** Single-particle energies of neutron states of the $^{90,92,94,96}$Zr nuclei: (closed symbols, connected by dashed lines in order to guide the eye) experimental data and (open symbols) results of the calculations with the dispersive optical potential.

### $n + {}^{100,112,116,118,120,124,132}$*Sn Systems*

Tin has ten stable isotopes—the largest number in relation to other isotopes. Therefore, the tin isotopes that are magic in protons ($Z = 50$) are a unique object for studying changes in the parameters of the nuclear structure as the number of neutrons in a nucleus increases.

To a high precision, the experimental values $E^{\rm expt}_{nlj}$ obtained in [21, 22] by the matching method for neutron states in the vicinity of the Fermi energy $E_{\rm F}$ in the stable isotopes $^{112,116,118,120,124}$Sn depend linearly on the mass number $A$. In [23], this circumstance was used to perform a linear extrapolation of the data in question and to obtain the evaluated energies $E^{\rm ev}_{nlj}$ for neutron states of the unstable nuclei $^{100,132}$Sn

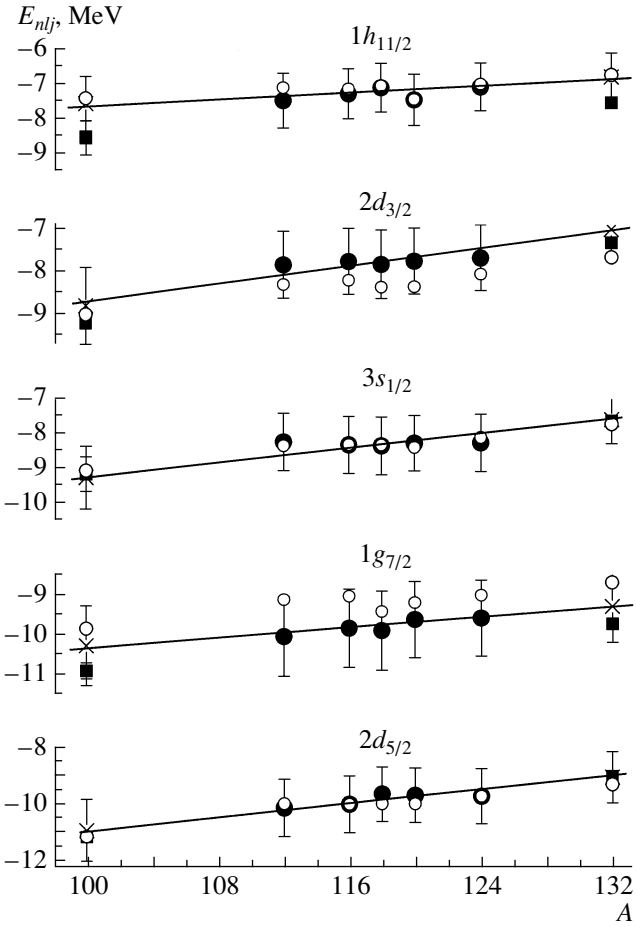


**Fig. 3.** Single-particle energies of neutron states in the $^{100,112,116,118,120,124,132}$Sn nuclei: (closed circles) experimental data obtained by the matching method, (closed squares) data from [24, 25], and (open circles) results of the calculation with the dispersive optical potential. The solid line represents a linear extrapolation.

featuring the traditional magic numbers of $N = 50$, 82 and $Z = 50$. The evaluated energies $E^{\rm ev}_{nlj}$ proved to be close to data obtained in [24, 25] for the $^{100,132}$Sn nuclei from the schemes of decay of neighboring nuclei. We used the energies $E^{\rm expt}_{nlj}$ and $E^{\rm ev}_{nlj}$ to construct the neutron dispersive optical potential for the $^{100,112,116,118,120,124,132}$Sn nuclei, which make it possible to demonstrate the potential of the method for determining the parameters of the dispersive optical potential of our present study for the isotopic chain as the number of neutrons $N$ increases by 32.

In order to evaluate the energies of the $1s_{1/2}$ neutron states in the $^{100}$Sn and $^{132}$Sn nuclei, we used the following information. The energy of the $1s_{1/2}$ neutron state is known from experiments for the $^{90}_{40}$Zr$_{50}$ nucleus, which is the nearest neighbor in $Z$: $E_{1s_{1/2}} = -70.0 \pm 2.3$ MeV [11]. Since $^{100}_{50}$Sn$_{50}$ also contains 50 neutrons, the energy of the $1s_{1/2}$ state in $^{100}_{50}$Sn$_{50}$ can be estimated by comparing the neutron single-particle energies for $^{100}_{50}$Sn$_{50}$ and $^{90}_{40}$Zr$_{50}$. The mean shift in energy between $E^{\rm ev}_{nlj}$ in $^{100}$Sn and $E^{\rm expt}_{nlj}$ in $^{90}$Zr is about 4 MeV. Therefore, we estimated the neutron-state energy in $^{100}_{50}$Sn$_{50}$ at $-75$ MeV. In order to estimate $E_{1s_{1/2}}$ in the $^{132}_{50}$Sn$_{82}$ nucleus, we made use of regularities in the results of the calculations of $E_{1s_{1/2}}$ for tin isotopes from $^{100}$Sn to $^{132}$Sn within the relativistic mean-field model. According to [12], the energies of the $1s_{1/2}$ neutron states in the $^{100}$Sn and $^{132}$Sn nuclei differ by 3.5 MeV. Therefore, we set the value of $E_{1s_{1/2}}$ for the $^{132}$Sn nucleus to $-72$ MeV. In order to estimate $E_{1s_{1/2}}$ for the $^{112,116,118,120,124}$Sn nuclei, we assumed that the energy $E_{1s_{1/2}}$ is a linear function of the number of neutrons in nuclei and changes from $-75$ MeV for $^{100}$Sn to $-72$ MeV for $^{132}$Sn.

The Fermi energy $E_{\rm F}$ for the doubly magic nucleus $^{100}$Sn was determined as the half-sum of the

energies of the $1g_{7/2}$ and $2d_{5/2}$ states, while the Fermi energy for the doubly magic nucleus $^{132}$Sn was determined as the half-sum of the energies of the $2d_{3/2}$ and $2f_{7/2}$ states. The experimental occupation numbers $N_{nlj}^{\text{expt}}$ [21, 22] for neutron states in the $^{112,116,118,120,124}$Sn nuclei exhibit a strongly smeared Fermi surface; because of correlation effects, their values differ markedly from zero and one, which are characteristic of the single-particle shell model. In order to determine the Fermi energy $E_{\text{F}}$ in these nuclei, we made use of formula (2) of Bardeen–Cooper–Schrieffer theory. The parameters of the dispersive optical potential (see [21–23]) that were found by the method used in our present study change insignificantly with increasing $N$ in nuclei. Figure 3 shows that the calculated energies $E_{nlj}^{\text{DOP}}$ are in good agreement with the experimental values $E_{nlj}^{\text{expt}}$ and with the evaluated data $E_{nlj}^{\text{ev}}$ for neutron states of the $^{100,112,116,118,120,124,132}$Sn nuclei.

## 4. CONCLUSIONS

In order to investigate the single-particle shell structure of magic and near-magic spherical nuclei and nuclei close to them, both stable and unstable ones, a general method has been proposed for constructing a dispersive optical potential. The method is aimed at calculating single-particle properties of spherical nuclei and nuclei close to them, including unstable neutron-rich and neutron-deficient nuclei.

The proposed method has been applied to determining the dispersive optical potential for the $n + {}^{40,42,44,46,48}$Ca, $^{46,48,50}$Ti, $^{50,52,54}$Cr, $^{54,56,58}$Fe, $^{56,58,60,62,64,68}$Ni, $^{84,86,88}$Sr, $^{90,92,94,96}$Zr, and $^{100,112,116,118,120,124,132}$Sn and the $p + {}^{46,48,50}$Ti, $^{50,52}$Cr, $^{54,56}$Fe, and $^{92,94,96}$Zr systems, and single-particle energies have been calculated on the basis of this method. The results have been found to be in agreement with experimental data within the errors in them.

The experimental isotonic and isotopic dependences of single-particle energies have been determined for $20 \leqslant Z \leqslant 28$ nuclei in which the number of neutrons $N$ was close to 28, as well as for $Z = 50$ nuclei. The use of these dependences has made it possible to evaluate the energies $E_{nlj}$ for several neutron states in stable titanium, chromium, and iron isotopes and in the unstable nuclei of $^{68}$Ni and $^{100,132}$Sn and to find the dispersive optical potential for these nuclei.

We have shown that magic properties of stable nuclei having previously known magic numbers of neutrons $N = 20$, 28, 50 ($^{40,48}$Ca, $^{50}$Ti, $^{52}$Cr $^{54}$Fe, $^{56}$Ni, $^{88}$Sr); unstable $N = 50$ and 82 nuclei ($^{100,132}$Sn); and nuclei that are candidates for new magic nuclei having $N = 34$ and $Z = 20$ ($^{54}$Ca), $N = 40$ and $Z = 28$ ($^{68}$Ni), and $N = 56$ and $Z = 40$ ($^{96}$Zr) manifest themselves in the dynamics of single-particle spectra of neutron states. On the basis of the method developed here for constructing a dispersive optical potential, the observed regularities have been described within the experimental errors.

## ACKNOWLEDGMENTS

This work was funded by a grant (no. 485.2008.2) from the President of the Russian Federation for support of leading scientific schools and within the State Contract no. 02.513.12.0046.

## REFERENCES

1. C. Mahaux and R. Sartor, Adv. Nucl. Phys. **20**, 1 (1991).
2. J. P. Delaroche, Y. Wang, and J. Rapaport, Phys. Rev. C **39**, 391 (1989).
3. C. Mahaux and R. Sartor, Nucl. Phys. A **503**, 525 (1989).
4. I. N. Boboshin, V. V. Varlamov, B. S. Ishkhanov, and I. M. Kapitonov, Nucl. Phys. A **496**, 93 (1989).
5. G. Mairle, M. Seeger, M. Ermer, et al., Phys. Rev. C **47**, 2113 (1993).
6. A. J. Koning and J. P. Delaroche, Nucl. Phys. A **713**, 231 (2003).
7. R. L. Varner, W. J. Thompson, T. L. McAbee, et al., Phys. Rep. **201**, 57 (1991).
8. R. F. Carlson, At. Data Nucl. Data Tables **63**, 93 (1996).
9. E. A. Romanovsky, O. V. Bespalova, T. P. Kuchnina, et al., Yad. Fiz. **61**, 37 (1998) [Phys. At. Nucl. **61**, 32 (1998)].
10. S. S. Volkov, A. A. Vorob'ev, O. A. Domchenkov, et al., Yad. Fiz. **52**, 1339 (1990) [Sov. J. Nucl. Phys. **52**, 848 (1990)].
11. A. A. Vorob'ev, Yu. V. Dotsenko, A. A. Lobodenko, et al., Yad. Fiz. **58**, 1923 (1995) [Phys. At. Nucl. **58**, 1817 (1995)].
12. S. Typel and H. H. Wolter, Nucl. Phys. A **656**, 331 (1999).
13. C. Mahaux and R. Sartor, Nucl. Phys. A **528**, 253 (1991).
14. M. Honma, Phys. Rev. S **65**, 061301(R) (2002).
15. O. V. Bespalova, I. N. Boboshin, V. V. Varlamov, et al., Yad. Fiz. **68**, 216 (2005) [Phys. At. Nucl. **68**, 191 (2005)].
16. O. V. Bespalova, I. N. Boboshin, V. V. Varlamov, et al., Yad. Fiz. **71**, 37 (2008) [Phys. At. Nucl. **71**, 36 (2008)].
17. H. Grawe and M. Lewitowicz, Nucl. Phys. A **693**, 116 (2001).
18. O. V. Bespalova, I. N. Boboshin, V. V. Varlamov, et al., Izv. Akad. Nauk, Ser. Fiz. **70**, 694 (2006).

19. O. V. Bespalova, I. N. Boboshin, V. V. Varlamov, et al., Yad. Fiz. **70**, 824 (2006) [Phys. At. Nucl. **70**, 796 (2006)].
20. Y. Wang, C. C. Foster, R. D. Polak, et al., Phys. Rev. C **47**, 2677 (1993).
21. O. V. Bespalova, I. N. Boboshin, V. V. Varlamov, et al., Izv. Akad. Nauk, Ser. Fiz. **69**, 678 (2005).
22. O. V. Bespalova, I. N. Boboshin, V. V. Varlamov, et al., Izv. Akad. Nauk, Ser. Fiz. **69**, 116 (2005).
23. O. V. Bespalova, I. N. Boboshin, V. V. Varlamov, et al., Izv. Akad. Nauk, Ser. Fiz. **71**, 448 (2007).
24. R. Schubart, H. Grawe, J. Heese, et al., Z. Phys. A **352**, 373 (1995).
25. D. Vretenar, T. Niksic, and P. Ring, Phys. Rev. B **65**, 024321-1 (2002).

*Translated by A. Isaakyan*